Ion Partitioning between Charged Micropores and Bulk Electrolyte Solution. Mixtures of Mono- and Divalent Counterions and Monovalent Co-Ions

B. Jamnik and V. Vlachy*

Contribution from the Department of Chemistry, University of Ljubljana, Ljubljana, Slovenia

Received February 1, 1995[⊗]

Abstract: The exclusion of mixed electrolytes from charged and uncharged cylindrical capillaries is studied using the grand canonical Monte Carlo method and the Poisson−Boltzmann equation. Concentration profiles inside the capillary, the Donnan exclusion coefficient, the separation factor, and concentration fluctuations were evaluated for a system with a mixture of divalent and monovalent counterions and monovalent co-ions. The electrolyte is treated in the restrictive primitive model approximation. All these quantities are studied as a function of the composition of the bulk external electrolyte. The calculations apply to a range of surface charge densities and to two values of the total ionic strength. The simulation results are compared with the predictions of the Poisson−Boltzmann approximation and the ideal Donnan theory. Both approximate theories grossly overestimate the ability of a micropore to exclude electrolytes. For higher concentrations of divalent counterions present in the system the Poisson−Boltzmann theory yields incorrect results. We present a comparison with the experimental data for charged membranes immersed in a mixed $KCl/CaCl_2$ solution.

1. Introduction

The problem of electrolyte exclusion from porous media is of great interest in chemical science and considerable effort has been devoted toward understanding the physicochemical properties of such systems. During the past ten years advances in the statistical mechanical theory[1] have led to renewed attack on this problem. Recent progress in the theory of electrolytes in micropores has been reviewed in refs 2 and 3.

The prediction of the partitioning of the positive and negative ions of an electrolyte between a charged (or uncharged) micropore and the isotropic electrolyte phase is important for better understanding and designing of several chemical and engineering processes.[2] One example of the industrial importance is the "reverse osmosis", which forms the basis of the technological processes for the desalination of water.[4] Further, these studies are important in connection with the separation methods, such as the countercurrent electrolysis method or convective electrophoresis in porous membranes.[5] Another relevant example is a study of equilibrium between electrolyte and the ion-exchange resin.[6]

Traditionally the phenomenon of ion partitioning has been understood on the basis of the classical Donnan equilibrium.[7] Due to the charged groups on the internal walls, there is an excess of counterions next to the surface, while the co-ions are partially excluded from this region. As a result, the electrolyte concentration within the capillary is often reduced below the bulk value. Experimental results indicate[8−13] that rejection of the 1:1 electrolyte increases by with an increase in the surface charge (capacity) of a micropore. Also, greater rejection is observed for dilute solutions. The exclusion coefficient, here defined by eq 1, is a convenient measure of this effect for both charged and uncharged capillaries.

$$\Gamma = \frac{c_- - \langle c_- \rangle}{c_-} \tag{1}$$

In eq 1, c_- denotes the concentration of co-ions in the bulk (external) electrolyte and $\langle c_- \rangle$ is the average concentration of co-ions in a micropore.

The simplest description of ionic effects in these systems provides the ideal Donnan theory.[7] The assumptions of the theory are as follows: (i) ion activities inside and outside the micropore are equal to their concentrations, and (ii) electroneutrality holds inside and outside the capillary. The theory greatly overestimates the actual rejection coefficient as, for example, seen in Figure 1. The rejection of electrolyte solutions with multivalent counterions has also been studied.[13] The experimental evidence suggests that the opposite effect, namely the enrichment of electrolyte (not a rejection), may take place in systems with multivalent counterions. The Donnan theory cannot explain these results, as it cannot explain an electrolyte exclusion from uncharged microcapillaries.[14]

A more detailed model of the electrolyte exclusion is based on the Poisson−Boltzmann equation.[3,15−22] Although the

[⊗] Abstract published in *Advance ACS Abstracts,* July 1, 1995.

(1) Henderson, D. *Fundamentals of Inhomogeneuos Fluids*; Marcel Dekker: New York, 1992.
(2) Vlachy, V.; Haymet, A. D. J. *Aust. J. Chem.* **1990**, *43*, 1961.
(3) Lozada-Cassou, M. In *Fundamentals of Inhomogeneuos Fluids*; Henderson, D., Ed.; Marcel Dekker: New York, 1992; p 303.
(4) McKelvey, J. G.; Spiegler, K. S.; Wyllie, M. R. J. *Chem. Eng. Prog., Symp. Ser.* **1959**, *55*, 199.
(5) Higa, M.; Kira, A.; Tanioka, A.; Miyasaka, K. *J. Chem. Soc., Faraday Trans.* **1993**, *89*, 3433 and references therein.
(6) Helfferich, F. *Ion Exchange*; McGraw Hill: New York, 1962.
(7) Donnan, F. *Z. Electrochem.* **1911**, *17*, 572.
(8) Marcinkowsky, A. E.; Kraus, K. A.; Phillips, H. O.; Johnson, J. S.; Shor, A. J. *J. Am. Chem. Soc.* **1966**, *88*, 5744.
(9) Jacazio, G.; Probstein, R. F.; Sonin, A. A.; Young, D. *J. Phys. Chem.* **1972**, *76*, 4015.
(10) Westermann-Clark, G. B.; Anderson, J. L. *J. Electrochem. Soc.* **1983**, *130*, 839.
(11) Hijnen, H. J. M.; van Daalen, J.; Smit, J. A. M. *J. Colloid Interface Sci.* **1985**, *107*, 525.
(12) Dubois, M.; Zemb, T.; Belloni, L.; Delville, A.; Levitz, P.; Setton, R. *J. Chem. Phys.* **1992**, *96*, 2287.
(13) Kraus, K. A.; Marcinkowsky, A. E.; Johnson, J. S.; Shor, A. J. *Science* **1966**, *151*, 194.
(14) Vlachy, V.; Haymet, A. D. J. *J. Electroanal. Chem.* **1990**, *283*, 77.

0002-7863/95/1517-8010$09.00/0

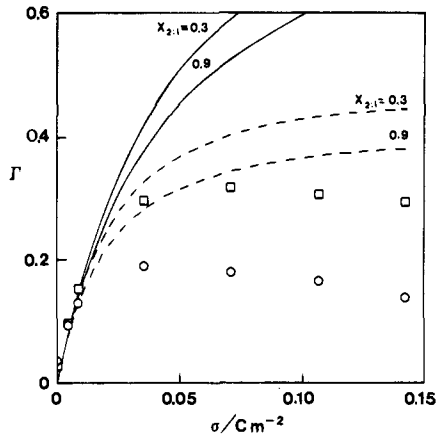

Figure 1. Exclusion parameter Γ as a function of the surface charge density σ for 2:1 + 1:1 electrolyte inside the capillary. Ionic strength of the equilibrium bulk solution is $I = 0.1456$ mol/dm^3 and the composition parameter is $x_{2:1} = 0.3$ (squares) and 0.9 (circles), respectively. Results are given for the Poisson–Boltzmann equation (dashed lines), and for the ideal Donnan theory (solid lines).

Poisson–Boltzmann approximation has been successful in describing various experimental results, question remains as to its validity, one reason being the statistical-mechanical approximations of the theory.[23] In our previous papers[2,14,24,25] the exclusion of electrolyte from charged and uncharged capillaries was studied using the Poisson–Boltzmann equation and the grand canonical Monte Carlo simulation technique. The structure and thermodynamics were examined as a function of the various model parameters for symmetric (1:1 and 2:2)[24] and for charge asymmetric (1:2 and 2:1) model electrolytes.[25] The simulation results show that there are a number of features which cannot be reproduced by the Poisson–Boltzmann approximation—in particular it cannot be used safely if divalent counterions are present in the system. The present paper extends this work to biologically more interesting systems, i.e. to charge asymmetric mixtures with a common ion. One example of such a system is a mixture of $CaCl_2$ and KCl, but the molecular parameters used here do not correspond to any particular mixture. In our study the capillary is negatively charged, so negative ions (chlorine) are co-ions and positive ions are counterions. When the charge asymmetric mixtures are forced through the membrane, the divalent counterions are attracted more strongly than monovalent counterions and therefore the electrolyte composition inside the capillary differs from that in the bulk. The study is of relevance for many interesting phenomena, such as (i) transport of electrolyte across charged membranes,[5] (ii) ion-exchange equilibrium,[6,26] or (iii) swelling transition due to the Ca^{2+}/Na^+ exchange in gels.[27,28]

The outline of this paper is the following. After the introduction (Section 1), we briefly present the model and numerical methods (Section 2). The results for the excess chemical potential of the (bulk) isotropic mixtures are presented in Section 3. The Donnan exclusion coefficient, the local ionic distributions within a micropore, the separation factor, and the concentration fluctuations are reported in Section 4. The comparison with experimental results of Higa and co-workers[5] is presented in Section 5. Finally, the conclusions are summarized in Section 6.

2. Methods of Calculation

A. Model. The model used in this study has been described in several previous studies.[24,25] The porous material is pictured as a collection of equal cylindrical capillaries of radius R_c, which do not interact with each other (cf. Figure 1 of ref 24). The capillary is assumed to be very long so that end effects are unimportant and except for the negative charge being smeared on the inner surfaces otherwise inert. The surface charge density is defined to be

$$\sigma = -\frac{|ze_0|}{2\pi R_c h} \tag{2}$$

where ze_0 is the charge and h is the link of the micropore. The ions in the system are treated as charged hard spheres of diameter a, and they can approach the surface only up to the distance $a/2$, i.e. the centers of ions are distributed within the cylindrical volume of radius $R = R_c - a/2$. The model porous material is treated as a dielectric continuum with the relative permittivity ϵ_r, and the dielectric image effects due to a difference in the permittivity of ions and other constituents of the system are ignored here. The electrolyte in the micropore is assumed to be in equilibrium with an external (bulk) electrolyte solution of composition $x_{2:1} = I_{2:1}/I$, where $I_{2:1}$ is the ionic strength of the 2:1 electrolyte and $I = {}^1/_2\sum_i c_i z_i^2$, is the total ionic strength.

B. Grand Canonical Monte Carlo Method. An extensive description of the grand canonical Monte Carlo (GCMC) method is given in ref 29. During a simulation, the configurational states are sampled at constant chemical potential μ and temperature T, while the number of ions inside the capillary fluctuates. The first step in the procedure is canonical (the number of ions is fixed during the step): a randomly chosen ion is moved into a new random position in the cell. The attempted move is accepted with probability f_{ij}

$$f_{ij} = \min[1, exp(-\beta(U_j - U_i))] \tag{3}$$

where U_i is the configurational energy of state i (old position of the ion), U_j is the configurational energy of state j, and as usual $\beta = (k_B T)^{-1}$, where k_B is the Boltzmann constant and T is the absolute temperature. In the next step a random decision is made to attempt either the insertion or the deletion of a neutral combination of ions $\nu = \nu_- + \sum\nu_{+x}$, where ν_{+x} and ν_- are the numbers of randomly chosen mono- and divalent cations and negative ions, respectively. The acceptance probabilities for addition and for deletion of ν ions ($CaCl_2$ or KCl combination) from a micropore are given by eq 4.

$$f_{ij} = \min[1, Y_{ij}], \quad \text{for addition}$$

$$f_{ji} = \min\left[1, \frac{1}{Y_{ij}}\right], \quad \text{for deletion} \tag{4}$$

After calculating the energies U_i and U_j, the transition probability f_{ij} from the state i with the number of anions N_{i^-} and cations $N_{i^{+x}}$ to the state j, where $N_{j^-} = N_{i^-} + \nu_-$ and $N_{j^{+x}} = N_{i^{+x}} + \nu_{+x}$, is given by

$$Y_{ij} = \frac{N_{i^-}! \prod N_{i^{+x}}!}{N_{j^-}! \prod N_{j^{+x}}!} \exp[B - \beta(U_j - U_i)] \tag{5}$$

The sign $\prod$ denotes a product over the positive species in the system: $\prod N_{i^{+x}}! = N_{i^{+2}}! N_{i^{+1}}!$. Parameter B in eq 5, $B = \beta(\mu - \mu_{ideal}) + \ln(N_-^{\nu_-} \prod N_{+x}^{\nu_{+x}})$, is related to the excess chemical potential of the bulk electrolyte with ionic concentrations N_{+x}/V and N_-/V.

(15) (a) Kobatake, Y. *J. Chem. Phys.* **1958**, *28*, 146. (b) Kobatake, Y. *J. Chem. Phys.* **1958**, *28*, 442.
(16) Dresner, L.; Kraus, K. A. *J. Phys. Chem.* **1963**, *67*, 990.
(17) Dresner, L. *J. Phys. Chem.* **1963**, *67*, 1635.
(18) Morrison, F. A., Jr.; Osterle, J. F. *J. Chem. Phys.* **1965**, *43*, 2111.
(19) Dolar, D.; Vlachy, V. *Vestn. Slov. Kem. Drus.* **1981**, *28*, 327.
(20) Vlachy, V.; McQuarrie, D. A. *J. Phys. Chem.* **1986**, *90*, 3248.
(21) Marčelja, S.; Quirk, J. P. *Langmuir* **1992**, *8*, 2778.
(22) Lo, W. Y.; Chan, K. Y.; Mok, K. L. *J. Phys. Condens. Matter* **1994**, *6*, 145.
(23) Fixman, M. *J. Chem. Phys.* **1979**, *70*, 4995.
(24) Vlachy, V.; Haymet, A. D. J. *J. Am. Chem. Soc.* **1989**, *111*, 477.
(25) Jamnik, B.; Vlachy, V. *J. Am. Chem. Soc.* **1993**, *115*, 660.
(26) Barak, P. *J. Colloid Interface Sci.* **1989**, *133*, 479.
(27) Tasaki, I.; Byrne, P. M. *Biopolymers* **1994**, *34*, 209.
(28) Siegel, R. *Adv. Polym. Sci.*, **1993**, *109*, 234.
(29) Valleau, J. P.; Cohen L. K. *J. Chem. Phys.* **1980**, *72*, 5935.

Table 1. GCMC and HNC Results for the Charge Asymmetric Mixtures of the Primitive Model Electrolytes[a]

I (mol dm^{-3})	$x_{2:1}$	$-\ln \gamma_{\pm 2:1}$	$-\ln \gamma_{\pm 1:1}$	$-\beta E$	$S(0)$
		GCMC			
0.1496	0.679	0.576	0.275	0.485	1.16
0.2965	0.635	0.691	0.312	0.580	1.12
		HNC			
0.1496	0.679	0.580	0.275	0.484	1.145
0.2965	0.635	0.695	0.315	0.580	1.12

[a] The electrolyte concentrations are $c_{2:1} = 0.0338$ mol/dm^3 and $c_{1:1} = 0.0481$ mol/dm^3 for $x_{2:1} = 0.679$ and $c_{2:1} = 0.0627$ mol/dm^3 and $c_{1:1} = 0.1083$ mol/dm^3 for $x_{2:1} = 0.635$. $c_{2:1}$ is the concentration of the 2:1 electrolyte in the bulk mixture and $x_{2:1}$ is the concentration parameter, defined as $x_{2:1} = I_{2:1}/I$, where $I_{2:1}$ is the ionic strength of the 2:1 electrolyte and I is the total ionic strength. $\gamma_\pm$ is the mean activity coefficient, βE is the reduced configurational energy and $S(0)$ is defined by eq 11. Averages in the simulations are collected over 5×10^6 configurations.

Table 2. The HNC Results as a Function of the Composition $x_{2:1}$ ($I = 0.1496$ mol/dm^3)

$x_{2:1}$	$c_{2:1}$ (mol dm^{-3})	$c_{1:1}$ (mol dm^{-3})	$-\ln \gamma_{\pm 2:1}$	$-\ln \gamma_{\pm 1:1}$
0		0.1496		0.254
0.3	0.0150	0.1047	0.577	0.263
0.9	0.0449	0.0150	0.583	0.284
1.0	0.0499		0.585	

Table 3. The HNC Results as a Function of the Composition $x_{2:1}$ ($I = 0.2965$ mol/dm^3)

$x_{2:1}$	$c_{2:1}$ (mol dm^{-3})	$c_{1:1}$ (mol dm^{-3})	$-\ln \gamma_{\pm 2:1}$	$-\ln \gamma_{\pm 1:1}$
0		0.2965		0.279
0.3	0.0296	0.2075	0.685	0.295
0.9	0.0889	0.0296	0.705	0.333
1.0	0.0988		0.710	

The grand canonical Monte Carlo method (cf. eq 5) requires advance knowledge of the excess chemical potential of the bulk electrolyte phase. The data for mixtures of electrolytes with asymmetric charge are, to our knowledge, unavailable in literature and we ran our own simulations of the bulk electrolyte. The hypernetted-chain (HNC) integral equation[30] has been used to interpolate between the systems of various composition. The GCMC and HNC results for the activity coefficient of bulk electrolyte mixtures are reported in Tables 1–3.

C. Poisson–Boltzmann Equation. The Poisson–Boltzmann equation for the cylindrical symmetry reads

$$\frac{1}{r}\frac{d}{dr}\left[r\frac{d\psi}{dr}\right] = -\frac{\varrho_e}{\epsilon_0\epsilon_r} \tag{6}$$

$$\varrho_e = z_{+1}e_0 n_{+1}(0)e^{-z_{+1}e_0\beta\psi} + z_{+2}e_0 n_{+2}(0)e^{-z_{+2}e_0\beta\psi} + z_{-}e_0 n_{-}(0)e^{-z_{-}e_0\beta\psi} \tag{7}$$

where $\psi(r)$ is the mean electrostatic potential at a distance r and $n_i(0)$ is the number concentration of ionic species i at $r = 0$. The boundary conditions are given by the Gauss law

$$\left(\frac{\partial\psi}{\partial r}\right)_{r=R_c} = -\frac{\sigma}{\epsilon_0\epsilon_r}$$

$$\left(\frac{\partial\psi}{\partial r}\right)_{r=0} = 0 \tag{8}$$

The Poisson–Boltzmann equation has been solved numerically for the mean electrostatic potential, using the so-called "shooting method".[31]

(30) (a) Rasaiah, J. C.; Friedman, H. *J. Chem. Phys.* **1968**, *48*, 2742. (b) Rasaiah, J. C.; Friedman, H. *J. Chem. Phys.* **1969**, *50*, 3965.

(31) Carnahan, B.; Luther, H. A.; Wilkes, J. O. *Applied Numerical Methods*; Wiley: New York, 1969.

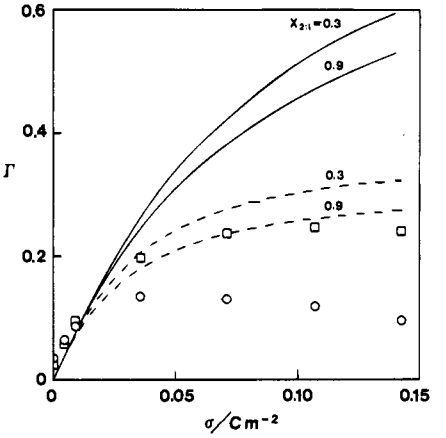

Figure 2. The same as for Figure 1, except that $I = 0.2965$ mol/dm^3.

Once the electrostatic potential is known, the ionic distributions and the average concentration of co-ions in a capillary $\langle c_- \rangle$ needed to determine the exclusion coefficient can be calculated.

3. Properties of "Bulk" Electrolytes

This section presents the grand canonical Monte Carlo and the HNC integral equation results for mixtures of the primitive model electrolytes. We are interested in charge asymmetric mixtures, i.e. mixtures of 1:1 and 2:1 electrolytes with a common ion. The ions are modeled as charged hard spheres of equal diameter (0.42 nm) in a solvent of uniform dielectric constant. The calculations apply to water-like solutions at 25 °C with the Bjerrum length $\lambda_B = \beta e_0^2/(4\pi\epsilon_0\epsilon_r)$, equal to 0.714 nm. The standard "minimum image" method for truncating the pair potential has proved to be sufficiently accurate under similar conditions and it is also used here. The mean activity coefficient, the excess energy, and the "osmotic compressibility" (concentration fluctuations) of bulk electrolyte (2:1 + 1:1 mixture) are given in Table 1. The HNC theory agrees well with the simulation results. For this reason, the HNC chemical potentials have been used in the GCMC simulations of electrolyte inside the micropore. The values of the "bulk" activity coefficient used in micropore simulations presented in Section 4 are given in Tables 2 and 3.

4. Electrolytes Inside Charged and Uncharged Capillaries

A. Exclusion Coefficient and Ionic Distributions. In this section we present numerical results for the primitive model electrolyte with a mixture of divalent and monovalent counterions and monovalent co-ions (2:1 and 1:1 electrolyte mixture) inside the negatively charged micropores. The surface charge density σ varies from zero (uncharged micropores) to 0.1425 C/m^2. The radius R ($=R_c - a/2$), of a cylindrical space available to ions is 4 nm, except for $\sigma = 0$ where micropores with two different values of R (1 and 4 nm) have been studied. The results apply to two values of the total ionic strength, i.e. to $I = 0.1496$ and 0.2965 mol/dm^3. The calculations have been carried out for several values of the composition parameter $x_{2:1}$.

Figures 1 and 2 show the Donnan exclusion coefficient Γ (eq 1), as a function of the surface charge density for $x_{2:1} = 0.3$ and 0.9 and for two values of the total ionic strength I. The Monte Carlo exclusion coefficient (symbols) first increases and after reaching a maximum value decreases as the charge on the surface is increased further. Similar behavior has been noticed for aqueous solutions of 2:2 and 2:1 electrolytes (divalent counterions) in micropores.[24,25] For low concentrations of divalent counterions in the bulk electrolyte ($x_{2:1} = 0.3$), Γ

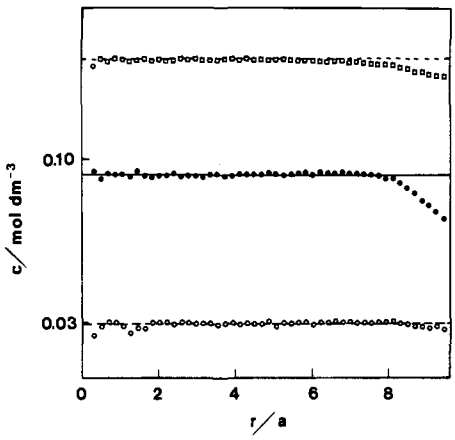

Figure 3. The GCMC results for the local concentrations of co-ions (squares) and divalent (solid circles) and monovalent counterions (open circles) inside the uncharged micropore. The lines denote ionic concentrations in an external solution (co-ions, short dashed line; monovalent counterions, dashed line; divalent counterions, solid line). The values of other parameters are $I = 0.2956$ mol/dm^3, $x_{2:1} = 0.9$, and $R = 4$ nm.

assumes higher values, while the position of a maximum is shifted toward higher charge densities.

The solid lines in Figures 1 and 2 are obtained using the (ideal) Donnan theory.[7] The starting point of the derivation is the electroneutrality condition for a capillary:

$$\sum_i z_i \langle c_i \rangle + c_x = 0 \qquad (9)$$

where c_x is the concentration of monovalent ions neutralizing the charge on the walls. Further, z_i is the valence and $\langle c_i \rangle = c_i K^{z_i}$ is the average concentration of the ionic species i inside the micropore. By assuming the activity coefficient of an ion inside the micropore is equal to that in a bulk mixture, the unknown K can be determined from eq 9 as described in ref 5. Once $\langle c_- \rangle$ is known, the exclusion parameter Γ can readily be calculated.

As shown in Figures 1 and 2, the ideal theory grossly overestimates the "exact" exclusion coefficients. The exclusion coefficients calculated via the Poisson–Boltzmann equation are presented with dashed lines in Figures 1 and 2. The Poisson–Boltzmann values of Γ are higher than those determined by the simulations. In summary, the two approximate theories suggest the charged micropores are considerably more efficient in excluding the electrolytes than is predicted by the computer simulations.

The nonzero values of Γ for uncharged capillaries (cf. Figure 1 and 2) are surprising only at first sight. In the next figures we present the concentration profiles of different ionic species inside uncharged micropores with $R = 4$ nm (Figure 3) and $R = 1$ nm (Figure 4). The value of the composition parameter of a bulk mixture is $x_{2:1} = 0.9$. In the immediate vicinity of the wall, the concentrations of all ionic species are reduced below the bulk value, due to the unbalanced interactions in this region.[32] The ions in contact with a wall, feel (in this model) no interaction from the side of the inert wall, merely from the subspace where other mobile ions are present. In simple terms, the isotropic ion atmosphere is distorted by the presence of the surface, and the distortion is larger for divalent ions. That is why the divalent counterions are, to a greater extent than the others, removed from the vicinity of the wall. Of course, the "excluded" counterions are followed by the co-ions in order to satisfy the electroneutrality condition inside the capillary. The Poisson–Boltzmann theory, as presented here, predicts no electrolyte exclusion under these conditions.

(32) Torrie, G. M.; Valleau, J. P.; Outhwaite, C. W. *J. Chem. Phys.* **1984**, *81*, 6297.

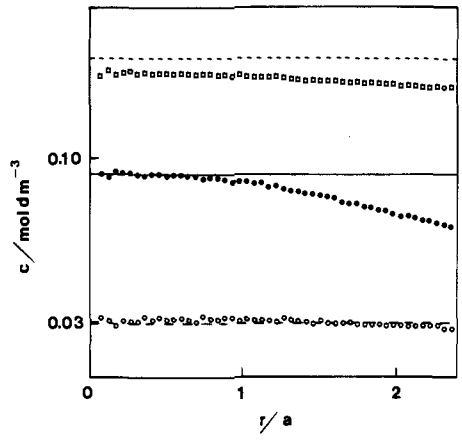

Figure 4. The same as for Figure 3, except for $R = 1$ nm.

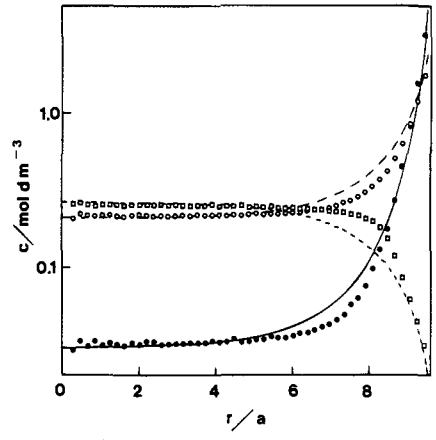

Figure 5. The same as for Figure 3, except for $\sigma = 0.1425$ C/m^2 and $x_{2:1} = 0.3$. Lines represent the Poisson–Boltzmann results. Notation as for Figure 3.

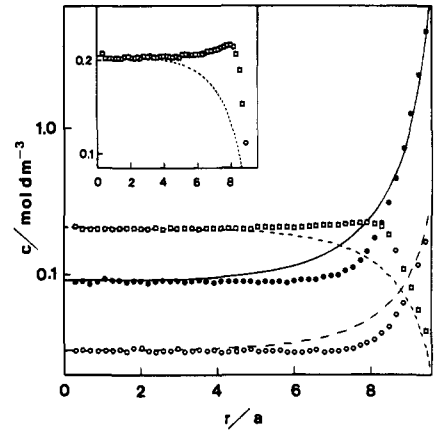

Figure 6. The same as for Figure 5, except for $x_{2:1} = 0.9$.

The next two figures show local concentrations of ions as a function of radial distance in the capillary, when a highly charged capillary ($\sigma = 0.1425$ C/m^2) is immersed into the bulk solution with $I = 0.2965$ mol/dm^3. The systems shown in Figures 5 and 6 differ in composition ($x_{2:1} = 0.3$ and 0.9), yet there are some general features which are common to both figures. *First*, the distribution of all species is considerably more uniform in the major part of a capillary than predicted by the Poisson–Boltzmann theory. *Second*, the Monte Carlo double layer is thinner than predicted by the Poisson–Boltzmann approximation. In a second case (Figure 6), where the divalent

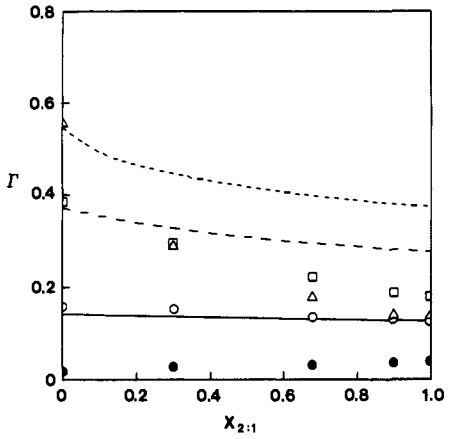

Figure 7. The exclusion parameter Γ as a function of the composition ($x_{2:1}$) of a bulk mixture with ionic strength 0.1496 mol/dm^3. The GCMC simulation results are denoted by symbols and the Poisson–Boltzmann results by lines: $\sigma = 0$ C/m^2, solid circles; $\sigma = 0.0089$ C/m^2, open circles and solid line; $\sigma = 0.0356$ C/m^2, squares and dashed line; $\sigma = 0.1425$ C/m^2, triangles and short dashed line.

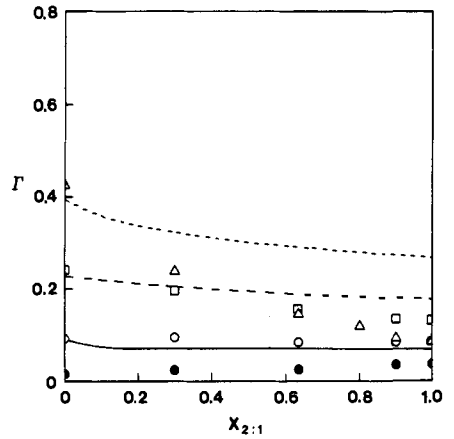

Figure 8. The same as for Figure 7, except for I = 0.2965 mol/dm^3.

counterions are present in an excess ($x_{2:1} = 0.9$), the electrical double layer extends only for about $r \approx 0.8$ nm from the surface of a capillary. *Third*, the average concentration of co-ions inside the capillary as obtained from simulation is considerably higher than predicted by the Poisson–Boltzmann equation. This is due to the strong correlation between co-ions and counterions, not accounted for by the classical Poisson–Boltzmann treatment. Strong correlation between the first layer of counterions and the co-ions is responsible for a distinct maximum in the concentration profile of co-ions, indicating that co-ions "see" from that distance a surface as a positively charged object. This effect has dramatic consequences for the exclusion coefficient—as seen in Figures 1 and 2, the ability of a micropore to exclude electrolyte is reduced well below the Poisson–Boltzmann value. Under conditions examined here, the concentration of co-ions and divalent counterions in contact with a charged wall appears to be slightly higher and that of the monovalent counterions is slightly lower than expected from the Poisson–Boltzmann calculation.

In this part we examine how the composition of the bulk electrolyte affects the Donnan coefficient. The results for Γ as a function of $x_{2:1}$ are, for several values of the surface charge density σ, shown in Figures 7 and 8. The conclusion is that the Donnan coefficient decreases with increasing concentration of divalent counterions in a mixture. The exception is the uncharged capillary—the situation in such systems has been discussed in relation to Figures 3 and 4. As expected, the

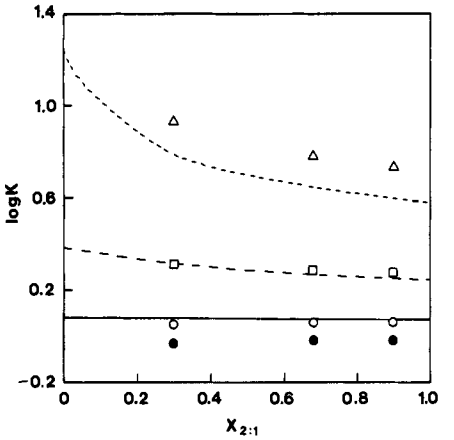

Figure 9. The separation factor K as a function of $x_{2:1}$ for $I = 0.1496$ mol/dm^3. Notation as for Figure 7.

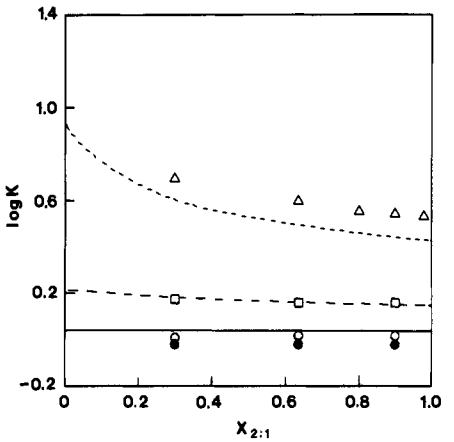

Figure 10. The same as for Figure 9, except for $I = 0.2965$ mol/dm^3.

micropore shows a greater ability to reject electrolytes for solutions of smaller ionic strength. It is clear from this calculation that the Poisson–Boltzmann theory has limited validity under these conditions.

B. Separation Factor. In this section the model of the charged capillary is used to predict separation factors for 2:1 + 1:1 electrolyte mixtures.[6,19] Figures 9 and 10 show the results for the separation factor K,[6] defined as

$$K = \frac{\langle c_2 \rangle / \langle c_1 \rangle}{c_2 / c_1} \tag{10}$$

as a function of $x_{2:1}$ for $I = 0.1496$ and 0.2956 mol/dm^3, respectively. In eq 10 $\langle c_2 \rangle$ and $\langle c_1 \rangle$ denote average concentrations of divalent and monovalent counterions in a micropore. Further, c_2 and c_1 are the concentrations of divalent and monovalent cations in an external solution. The Poisson–Boltzmann results are presented by lines and GCMC data by symbols. As expected, the separation efficiency increases with increasing σ. For mixtures inside the uncharged capillaries the separation factor is lower than unity. This is in agreement with the fact that divalent counterions are removed from the interior of uncharged micropore to a higher extent than the monovalent counterions. The micropore becomes more selective for divalent counterion if their fraction in an external solution is smaller. Similar behavior is observed when the total ionic strength of the external solution is reduced. All this is in qualitative agreement with the experimental results for the ion-exchange resins.

C. Concentration Fluctuations. An advantage of the GCMC method is that the particle number fluctuations can be

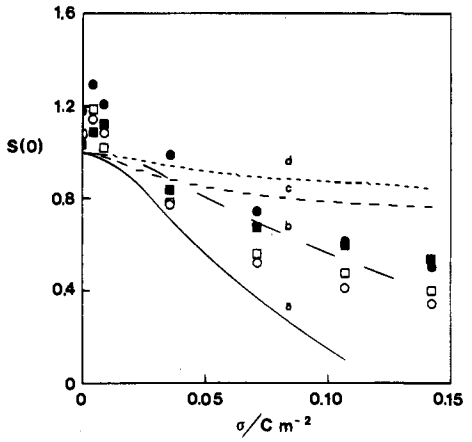

Figure 11. The concentration fluctuations as a function of the surface charge density. The GCMC simulation results are denoted by symbols and the Poisson–Boltzmann results by lines: $I = 0.1496$ mol/dm^3, $x_{2:1} = 0.3$—solid line (a), open squares; $I = 0.2965$ mol/dm^3, $x_{2:1} = 0.3$—long dashed line (b), solid squares; $I = 0.1496$ mol/dm^3, $x_{2:1} = 0.9$—dashed line (c), open circles; $I = 0.2965$ mol/dm^3, $x_{2:1} = 0.9$—short dashed line (d), solid circles.

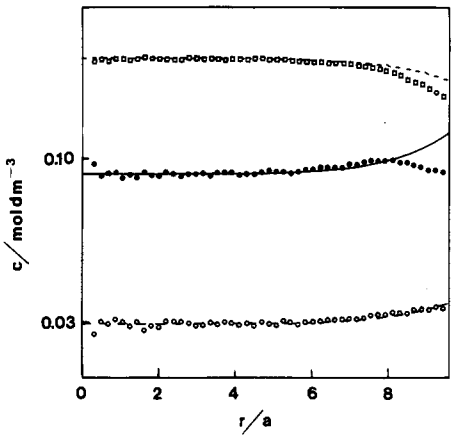

Figure 12. The same as for Figure 6, except for $\sigma = 0.00445$ C/m^2.

calculated directly.[33] The partial structure factors S_{ij} are in the long wavelength limit ($k \rightarrow 0$) related to the concentration fluctuations in a system via eq 11

$$\lim_{k\to 0} S_{ij}(k) = \frac{\langle N_i N_j\rangle - \langle N_i\rangle\langle N_j\rangle}{\sqrt{\langle N_i\rangle\langle N_j\rangle}} \tag{11}$$

For the concentration fluctuations in a multicomponent solution we define S(0) as

$$S(0) = \frac{1}{\varrho}\sum_{i,j}\sqrt{\varrho_i\varrho_j}\lim_{k\to 0} S_{ij}(k) \tag{12}$$

Here, $S(0)$ is an osmotic compressibility of the actual system, divided by the ideal gas value of the same quantity[33]

$$S(0) = k_B T\left(\frac{\partial\varrho}{\partial p}\right)_T \tag{13}$$

$S(0)$ is expected to decrease with an increase in the surface charge density of the capillary, and for the parameters of the simulation this holds true for $\sigma > 0.01$ C/m^2 (cf. Figure 11). A notable feature of Figure 11 is a maximum in $S(0)$ (GCMC results), which appears for small charge densities. The maximum can be explained in view of the ion–ion correlations next to the uncharged wall. For electrolyte enclosed in the inert capillary the concentration fluctuations are reduced below the bulk value. The correlation between ions in a capillary is quite important under these conditions, which accounts for the depletion of ions next to the charged surface. A fixed charge on the surface has to be nonzero in order to balance this effect, cf. Figure 12, which corresponds to a slight increase in $S(0)$. By further increase of the surface charge density, the concentration fluctuations are suppressed due to effects of the charged wall. In Figure 12, the concentration profiles of all three ionic species inside a micropore ($\sigma = 0.00445$ C/m^2, $x_{2:1} = 0.9$, $I = 0.2965$ mol/dm^3) are shown. $S(0)$ is a sensitive measure of interactions in electrolyte solutions; as seen from Figure 11 it depends on the surface charge density, total ionic strength, and composition of the external solution in a rather complicated manner. The lines in Figure 11 represent results obtained by the Poisson–Boltzmann equation, calculated as follows. First, the osmotic coefficient Φ has been calculated from eq 14,[20]

$$\Phi = \frac{\sum\varrho_i(0)}{\sum\langle\varrho_i\rangle} \tag{14}$$

where $\varrho_i(0)$ is the number density of the ionic species i in the middle of the capillary (at $r = 0$) and $\langle\varrho_i\rangle$ is the average number density in the isotropic solution. Then, from eq 13 we obtain

$$S(0) = \frac{1}{\Phi + \dfrac{\partial\Phi}{\partial\sum\varrho_i}\sum\varrho_i} \tag{15}$$

The Poisson–Boltzmann equation correctly predicts an increase of $S(0)$ when the ionic strength of the external solution is increased. The theory also gives qualitatively correct predictions for the osmotic compressibility when the fraction of divalent counterions in the external solution is low. The disagreement between the simulation and Poisson–Boltzmann results for $x_{2:1} = 0.9$ in the external mixture warns again that Poisson–Boltzmann theory should be used carefully when the observed ions carry more than one elementary charge.

5. Comparison with Experimental Data.

Comparison between experimental[5] and computational studies is presented in Figures 13 and 14. In the experimental study of Higa and co-workers,[5] the fixed charge is due to sulfonic groups on the internal walls and the electrolyte solution studied is an aqueous mixture of $CaCl_2$ and KCl. The capacity of the micropore (concentration of monovalent counterions that neutralize the wall-fixed charge) is 0.05 mol/dm^3. Since we do not have any information about the actual geometry of the micropores, the cylindrical symmetry is assumed ($R = 4.0$ nm), as described in Section 4. The ions are described as charged hard spheres of diameter 0.42 nm. In Figure 13 the average concentrations of all ionic species are plotted as a function of concentration of divalent ions in the external solution. The results apply to the equimolecular mixture of potassium and calcium chloride in the external electrolyte, [KCl]/[$CaCl_2$] = 1. The agreement between experimental data,[5] the Poisson–Boltzmann calculation, and GCMC results is (perhaps fortuitously) very good. This can be explained by a low value of the wall-fixed charge in the porous material used in the experimental study; the capacity 0.05 mol/dm^3 corresponds to $\sigma \approx 0.01$ C/m^2. As one can infer from Figure 1, this is a region where the Poisson–Boltzmann theory yields a good agreement

(33) March, N. H.; Tosi, M. P. *Coulomb Liquids*; Academic Press: London, 1984.

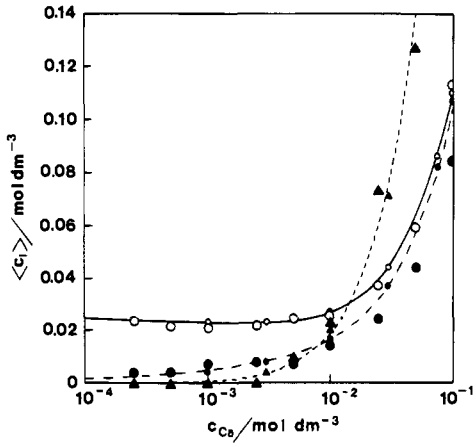

Figure 13. The average concentration of co-ions and counterions as a function of the concentration of divalent cations in the bulk solution; $[CaCl_2]/[KCl] = 1$. Lines represent the Poisson–Boltzmann results. The experimental[5] and the GCMC results are denoted by large and small symbols, respectively. Results are marked by solid triangles and short dashed lines for co-ions, by solid circles and dashed lines for monovalent counterions, and by open circles and a solid line for divalent counterions.

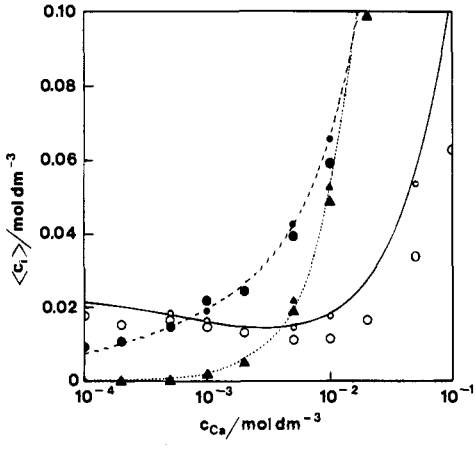

Figure 14. The same as for Figure 13, except for $[CaCl_2]/[KCl] = 0.2$.

with the simulation results. When the charged membrane is immersed in the solution with $[CaCl_2]/[KCl] = 0.2$ (Figure 14), the agreement is not as good. The average concentration of calcium ions inside the micropore, when plotted in Figure 14 as a function of the calcium concentration in the external solution, exhibits a broad minimum, hardly noticeable in the case of an equimolecular mixture of KCl and $CaCl_2$. Note, that average concentrations of counterions inside the micropore, determined by the cylindrical model, are higher than those observed in the experiment.

6. Conclusions

The partitioning of mono- and divalent counterions and monovalent co-ions between a charged micropore and external electrolyte solution has been investigated by the Poisson–Boltzmann and the grand canonical Monte Carlo method. One aim of this work was to determine the range of validity of the classical Poisson–Boltzmann approximation for these systems. The conclusions are in agreement with a recent study of the force between planar electrical double layers containing a counterion mixture, as presented by Feller and McQuarrie.[34] The Poisson–Boltzmann equation yields a good agreement with the simulation results for the pure monovalent case, i.e. if no divalent counterions are present in the solution. It is found that the presence of a small amount of divalent counterions significantly deteriorates the accuracy of the Poisson–Boltzmann theory. Mixtures containing a moderate to high fraction of divalent counterions show behavior that is characteristic for the pure divalent case, e.g., a maximum in the exclusion coefficient if plotted as a function of the surface charge density. Significant deviations from the Poisson–Boltzmann theory are found for all properties studied here.

The physical model applied in this work contains a number of approximations; most notably, it ignores the molecular nature of the solvent and the effect of the dielectric boundary. The long-ranged Coulomb forces may not be sufficient to describe in detail a complicated system such as the ion-exchange membrane studied in ref 5. Yet, before we include the solvation and other microscopic features in the model, a quantitatively correct description of the electric double layer for the primitive model electrolyte in the capillary is needed.

Acknowledgment. We are grateful to Dr. Mitsuru Higa for sending us the experimental results shown in Figures 13 and 14. This work was supported by the Ministry of Science and Technology of Republic of Slovenia.

JA950346N

(34) Feller, S. E.; McQuarrie, D. A. *Mol. Phys.* **1993**, 80, 721.